Gómez-Correa Luisa F (Orcid ID: 0009-0008-2091-2396)
Jaramillo-Hernández Camila (Orcid ID: 0009-0006-2213-9646)
Duque Alvaro (Orcid ID: 0000-0001-5464-2058)
Zuleta Daniel (Orcid ID: 0000-0001-9832-6188)

Author Manuscript

Gómez-Correa et al.

Canopy tree mortality depends on the proportion of crown exposed to sunlight, but this effect varies with species wood density

Luisa F. Gómez-Correa[1], Camila Jaramillo-Hernández[1], Alvaro Duque[1], Raquel Fernandes Araujo[2], Gabriel Arellano[3,4], Stuart J. Davies[5], Nicolas Castaño[6], Jörg Haarpaintner[7], Fabian Enßle[8,9], Daniel Zuleta[5*]

[1] Departamento de Ciencias Forestales, Universidad Nacional de Colombia Sede Medellín, Medellín, Colombia.

[2] Forest Global Earth Observatory, Smithsonian Tropical Research Institute, Balboa, Ancón, Panama

[3] Ecology and Evolutionary Biology, University of Michigan, Ann Arbor, MI, USA.

[4] Oikobit LLC, Albuquerque, NM, USA.

[5] Forest Global Earth Observatory, Smithsonian Tropical Research Institute, Washington, DC, USA.

[6] Herbario Amazónico Colombiano, Instituto Amazónico de Investigaciones Científicas SINCHI, Bogotá, Colombia.

[7] NORCE Climate and Environment - Norwegian Research Centre AS, Tromsø, Norway.

[8] Remote Sensing and Landscape Information Systems, University of Freiburg, Germany.

[9] Sustainable Development and Climate Hub, GAF AG, Germany.

* Corresponding author: dfzuleta@gmail.com

Received: _____; Revised:____(optional); Accepted:_____.

This is the author manuscript accepted for publication and has undergone full peer review but has not been through the copyediting, typesetting, pagination and proofreading process, which may lead to differences between this version and the Version of Record. Please cite this article as doi: 10.1111/btp.13258

This article is protected by copyright. All rights reserved.

Associate Editor: Jayashree Ratnam; Handling Editor: Robert Bagchi

Author Manuscript

Author Manuscript

ABSTRACT

Understanding what drives changes in tree mortality as well as the covariates influencing trees' response is a research priority to predict forest responses to global change. Here, we combined drone photogrammetry and ground-based data to assess the influence of crown exposure to light (relative to total crown area), growth deviations (relative to conspecifics), tree size, and species' wood density (as a surrogate for light-demanding and shade-tolerant life-history strategies) on the mortality of 984 canopy trees in an Amazon *terra firme* forest. Trees with lower wood density were less prone to die when their proportion of crown was more exposed to sunlight, but this relationship with relative crown exposure weakened and slightly reversed as wood density increased. Trees growing less than their species average had higher mortality, especially when the species' wood density decreased. The role of wood density in determining the survival of canopy trees under varying light conditions indicates differential responses of light-demanding versus shade-tolerant species. Our results highlight the importance of accounting for life-history strategies, via plant functional types, in vegetation dynamic models aiming to predict forest demography under a rapidly changing climate.

KEYWORDS: Amacayacu forest dynamics plot, drones, ForestGEO, growth rates, life-history strategies, light availability, tree survival, tropical forests.

Author Manuscript

RESUMEN

Comprender los factores que impulsan cambios en la mortalidad de los árboles así como las covariables que influencian la respuesta de éstos es una prioridad de investigación para predecir las respuestas de los bosques al cambio global. En este estudio, combinamos fotogrametría de drones y datos terrestres para evaluar la influencia de la exposición de la copa a la luz (relativo al área total de la copa), las desviaciones de la tasa de crecimiento (relativo a conespecíficos), el tamaño del árbol, y la densidad de la madera de la especie (como indicador de las estrategias de historia de vida demandantes de luz y tolerantes a la sombra) sobre la mortalidad de 984 árboles de dosel en un bosque de tierra firme de la Amazonía. Árboles de baja densidad de la madera fueron menos propensos a morir a mayor proporción de área de copa expuesta a la luz, pero esta relación con la exposición a la luz se debilitó y se invirtió ligeramente a medida que aumentó la densidad de la madera. Árboles que crecieron menos que el promedio de su especie presentaron mayor mortalidad, especialmente cuando la densidad de la madera decreció. El rol de la densidad de la madera en determinar la sobrevivencia de los árboles de dosel bajo diferentes condiciones de luz indica respuestas diferenciales de las especies demandantes de luz y tolerantes a la sombra. Nuestros resultados resaltan la importancia de tener en cuenta las estrategias de historia de vida, a través de los tipos funcionales de plantas, en los modelos dinámicos de vegetación que tienen como objetivo predecir la demografía de los bosques bajo un clima rápidamente cambiante.

PALABRAS CLAVE: bosques tropicales, disponibilidad de luz, drones, estrategias de historia de vida, ForestGEO, parcela permanente Amacayacu, sobrevivencia de árboles, tasas de crecimiento.

Author Manuscript

1. INTRODUCTION

Tree mortality influences forest carbon dynamics, functioning, and composition. Increases in tree mortality have been suggested as the main cause of the long-term decline in Amazon carbon stocks (Hubau *et al.* 2020), with consequences for global climate regulation (Friedlingstein *et al.* 2022). The multivariate nature of tree mortality and the relatively low number of trees dying every year make it a difficult process to understand, estimate, and ultimately predict (McMahon *et al.* 2019; McDowell *et al.* 2022). Understanding what drives changes in tree mortality as well as the covariates influencing trees' response is a critical research avenue, especially in the tropics, where the high species diversity results in multiple responses to any given factor (Bauman *et al.* 2022; Zuleta *et al.* 2022a).

Tree mortality is a multivariate process that arise from multiple factors (Franklin *et al.* 1987). Some of these factors are slow or chronic (e.g., increasing vapor pressure deficit) ('presses', Harris *et al.* 2018), while others can kill trees within a single season (e.g., drought, pest outbreak) or almost instantaneously (e.g., lightning, wind disturbances) ('pulses', Negrón-Juárez *et al.* 2017; Yanoviak *et al.* 2020). These factors are non-mutually exclusive and operate at the individual, species, and stand levels (e.g., Aleixo *et al.* 2019; Arellano *et al.* 2019; Esquivel-Muelbert *et al.* 2020; Zuleta *et al.* 2022a). At the species level, trees generally array on a continuum of resource allocation strategies highly determined by the species' dependency on light (i.e., the growth-mortality trade-off; Wright *et al.* 2010; Reich *et al.* 2014). Across this widely recognized life history trade-off, light-demanding, fast-growing species generally die faster than shade-tolerant, slow-growing species (Kobe *et al.,* 1995; Nascimento *et al.* 2005; Poorter *et al.* 2008; Rüger *et al.* 2012). The low mortality of shade-tolerant, slow-growing

Author Manuscript

species is attributed to their high investment in wood structure (i.e., high wood density), a key trait that provides mechanical support, hydraulic safety during droughts, and greater resistance to pests and pathogens (Augspurger & Kelly 1984; Hacke *et al.* 2001; Chave *et al.* 2009; Feeley & Zuleta 2022). Therefore, the general expectation is that fast-growing individuals will die more often than slow-growing individuals. Within species, however, trees that grow slower than conspecifics are more prone to die (Camac *et al.* 2018; Arellano *et al.* 2019; Russo *et al.* 2021). Tree individual deviations in growth rates relative to the species averages have been used as a general predictor of tree vigor and should be considered when studying factors involved in tree mortality (Chao *et al.* 2009; Bigler *et al.* 2004).

Resource availability, both aboveground and belowground, influences mortality at the individual level (Russo *et al.* 2005; Zuleta *et al.* 2017; Arellano *et al.* 2019). Light, as the fundamental source of energy for photosynthesis, constitutes one of the major resources for which trees compete (Wright 2002; Muller-Landau *et al.* 2006), with trees more exposed to light having higher survival rates (Herwitz *et al.* 2000). In fact, light-limitation has been found to be one of the most prevalent and impactful mortality risks across six tropical forests, even for trees larger than 10 cm in diameter (Zuleta *et al.* 2022a). Light availability has been generally proxied by tree size, with large trees expected to be more exposed to light than small trees (Araujo et al. 2020) and (all else being equal) die less often as a consequence of that key advantage. However, the size-dependence of mortality does not seem to be monotonic. Several studies report that these patterns highlight the size-dependency of tree mortality, where intermediate-size trees die less than both small and large trees (Rüger *et al.* 2011; Arellano *et al.* 2019; Gora & Esquivel-Muelbert 2021). Large and presumably sun-exposed trees can also be more likely to die because they are subjected to high evaporative demands, high winds, lightning, and have accumulated

Author Manuscript

more damage by living longer (Bennett *et al.* 2015; Yanoviak *et al.* 2020). However, deviations from these general expectations about size-dependence arise because of gap openness, crown damage, or light competition (Jucker *et al.* 2015; Zuleta *et al.* 2022b). For example, a tree of 5 cm diameter at breast height (DBH) located in a gap can have higher light availability than a tree of 30 cm DBH located in the mid-canopy.

Here, we assessed the influence of individual- and species-level factors on the mortality of canopy trees (those directly exposed to sunlight) in the Amacayacu Forest Dynamics Plot in Colombia, northwestern Amazon. Canopy trees contribute disproportionately to carbon stocks and species diversity (Lutz *et al.* 2018; Araujo *et al.* 2020; Piponiot *et al.* 2022) and their survival has been found to be strongly driven by extreme climatic events, wood density, successional position, and deciduousness (Aleixo *et al.* 2019). We used an orthomosaic, i.e., an orthorectified image produced by photogrammetric processing of photos captured by a Remotely Piloted Aircraft System (RPAS, also known as drone), and two censuses of the 25-ha plot to evaluate the main influence and interactions of crown exposure to light (relative to total crown area), individual deviations of growth rates, tree size, and species wood density on the survival of canopy trees between 2013 and 2019. Given the conspicuous importance of light in plant processes, we expect trees with higher proportions of their crown exposed to direct sunlight to die less compared to less sun-exposed trees. We also expect mortality to be lower for trees growing more than conspecifics and for intermediate-size trees compared to both larger and smaller trees. However, considering the evolutionary strategies of the species, we expect these main patterns to covary with species' life history (as proxied by wood density). For example, light-demanding species are expected to always benefit (i.e., higher growth and survival) from

being in highly illuminated conditions; whereas shade-tolerant species are expected to be less dependent on light (Cifuentes & Moreno 2022; Valladares & Niinemets 2008).

2. MATERIALS AND METHODS

2.1 Study area

This study was carried out at the 25 ha Amacayacu Forest Dynamics Plot (AFDP), located in the Amacayacu National Natural Park in Colombia (3°48'33" S and 70°16'04" W), northwestern Amazon. The AFDP is located on an undisturbed *terra firme* forest (Heijink *et al.* 2020). The plot is part of the Forest Global Earth Observatory (ForestGEO; Davies *et al.* 2021) and consists of 123,000 trees of 1,200 species (Duque *et al.* 2017). The mean annual temperature is 25.8°C, mean annual precipitation is 3,216 mm and mean relative humidity is 86% (Zuleta *et al.* 2020). The plot is located on tertiary sediments of Pebas geological formation, the elevation varies between 89 and 108 a.s.l with hilly and moderately dissected topography, and has poor soils, high acidity, and low base saturations due to the dominance of minerals such as kaolinite and quartz (Chamorro 1989; Zuleta *et al.* 2020).

2.2 Data collection and processing

We tested the role of species-adjusted tree growth rates (i.e., growth rate relative to conspecifics), tree size, relative crown exposure to light, and species wood density on the mortality of 984 canopy trees of 265 species (48 families) in 18 ha of the AFDP. We gathered these variables for each tree in 2013 and assessed their survival status in 2019. We defined canopy trees as those trees exposed to direct vertical light. Below, we described the methods to obtain each of these variables.

Author Manuscript

Author Manuscript

2.2.1 Forest censuses

The AFDP was established between April 2007 and December 2009, where all free-standing woody stems (i.e., trees, shrubs, palms, and tree ferns) with diameter at breast height (DBH) ≥ 1 cm were mapped, tagged, measured, and collected for species identification. The second and third censuses were carried out between October 2013 and March 2016 and between July 2019 and February 2022, respectively. During these full censuses, the survival of all trees was assessed, the DBH for surviving trees was recorded, and all new recruits were measured, tagged, mapped, and identified. The mean census intervals between the first and second census (2007-2013) and between the second and third census (2013-2019) were 6.7 (standard deviation (SD = 1.1) and 5.2 (D = 1.3) years, respectively. Voucher specimens were deposited and identified in the Herbario Amazónico Colombiano (COAH) of the Instituto Amazónico de Investigaciones Científicas SINCHI.

2.2.2 Species-adjusted tree growth rates (SA-GR)

To estimate the tree growth rate deviation from the species average (SA-GR), we first calculated the growth rates (g, cm yr^{-1}) of trees with DBH ≥ 1 cm across the two census intervals (from 2007 to 2013 and from 2013 to 2019) in the 25 ha of the AFDP as:

$$g = \frac{DBH_{final} - DBH_{initial}}{time_{final} - time_{initial}},$$

where $DBH_{initial}$ and DBH_{final} are the diameters at the breast height (cm) at $time_{initial}$ and $time_{final}$, respectively, for each census interval. If the diameters were not measured at 1.3 m height we calculated the corrected DBH using the following taper equation (Metcalf *et al.* 2009):

$$DBH_{corrected} = D^{\alpha(HOM - 1.3)},$$

where α is the tapering factor and HOM is the height (m) of measurement of diameter D (cm). The tapering factor α was estimated for each tree as (Cushman *et al.* 2021):

$$\alpha = 0.151 - 0.025 * log(D) - 0.02 * log(HOM) - 0.021 * log(WD) + site,$$

where WD is the wood density of the species (g cm^{-3}) and *site* takes the value of -0.00161 for the AFDP.

To remove errors in DBH measurements, we excluded trees with $g > 4$ cm yr^{-1} as well as measurements in which the DBH_{final} was > $4SD$ below the $DBH_{initial}$, where SD = (0.006214 * $DBH_{initial}$) + 0.9036 and corresponds to the standard deviation of repeated DBH remeasurements (Condit *et al.* 2004). Since the distribution of g is extremely right-skewed, we applied the modulus transformation on the growth rates, which reduces the skewness of the data and allows the inclusion of negative growth rates (Condit *et al.* 2017). The modulus-transformed growth rate (GR) was calculated as g^{Θ} for $g \geq 0$, and $-\{(-g)^{\Theta}\}$ for $g < 0$. We used a $\Theta = 0.4$ since this value minimized the skewness of the growth rates of trees in the AFDP across both census intervals (Figures S1, S2, S3). We used GR instead of relative growth rates because the latter depends on tree size (Figure S4).

Finally, we estimated the SA-GR (unitless) for each tree i of species j in our sample as:

$$Species\ adjusted\ GR_{i,j} = \frac{GR_{i,j} - mean(GR)_j}{standard\ deviation(GR)_j}.$$

We limited our analysis to species with at least 25 growth observations to avoid unreliable estimates due to lack of variability in rare species.

2.2.3 Tree size (log(DBH))

To estimate the effect of tree size on mortality, we calculated the corresponding DBH (cm) of each tree at the time of the RPAS flight as:

Author Manuscript

$$DBH_{flight} = DBH_{2007} + \left(g * \left(time_{flight} - time_{2007}\right)\right),$$

where DBH_{2007} is the DBH (cm) of the tree at $time_{2007}$ (first full census), g is its growth rate (cm yr^{-1}), and $time_{flight}$ is the date of the RPAS flight. This DBH was finally log-transformed to improve model fitting.

2.2.4 Relative crown exposure to light (RCEL)

To assess the influence of light availability on canopy tree mortality we derived an unitless metric calculated as (Figure 1):

$$RCEL = \frac{ECA}{CA},$$

where ECA is the vertically sun-exposed crown area (m^2), calculated from a canopy orthomosaic obtained from a remotely piloted aircraft system (RPAS) (*see below*); and CA is the total crown area (m^2) estimated from an allometric model based on DBH_{flight} (*see below*). RCEL indicates the proportion of total DBH-derived crown area of a tree that is exposed to vertical sunlight and, thus, varies from 0 to 1. Trees with RCEL values close to 1 are more exposed to vertical sunlight, whereas trees with RCEL values close to 0 are less exposed to sunlight. We excluded trees with an ECA greater than the upper confidence interval of the prediction of crown area (five trees) and truncated to RCEL = 1 those trees with RCEL > 1 (70 trees). Note that, ecologically, this metric cannot distinguish between the processes driving the actual crown area, therefore, trees with RCEL < 1 might either be shaded by other trees or have an incomplete crown due to damage or other factors. Overall, RCEL is a measure of resource acquisition relative to the potential resource acquisition for a tree of a given size, a proxy for the "payback" or "return" on the resource investment for any given tree.

Author Manuscript

Author Manuscript

2.2.5 Vertically sun-exposed crown area (ECA)

We obtained near-infrared (NIR) images of the AFDP canopy using a RPAS in December, 2013, right at the beginning of the second census. The aim of this flight was to characterize the conditions of canopy trees around the date in which trees were measured on the ground. We used a fixed-wing SenseFLY Ebee integrated with a camera Canon PowerShot ELPH 110 HS with 4.3 mm focal length and 16 mpx of photo resolution. The total number of photos taken were 264 and the flying altitude was 112 m. We processed the photos on the photogrammetry software Agisoft Photoscan (https://www.agisoft.com, v.0.9.1) and generated a 6 cm spatial resolution orthomosaic. The georeferencing accuracy was assessed in terms of the root mean square error, where the X, Y, and Z errors were 1.8, 0.7, and 13.5 m, respectively. The orthomosaic reproduces the real dimensions of tree crowns.

We delineated all identifiable crowns of living trees with DBH ≥ 10 cm based on the NIR image and assigned their corresponding tag (i.e., unique individual code of the plot) over 18 ha of the AFDP using QGIS software v.3.16.5 (QGIS Geographic Information System 2022). We carried out a semi-automated crown delineation in which we first segmented the orthomosaic into polygons using the *segmentation* function of Orfeo ToolBox (Grizonnet *et al.* 2017) with a minimum region size of 7000 pixels (25.2 m^2) and, then, manually edited these polygons to adjust them to the actual tree crowns. For each 20 m x 20 m plot quadrant, we first assigned and adjusted tree crowns for individuals with the biggest DBHs followed by the consecutively smaller DBHs because the probability of being in the canopy increases logistically with diameter (Araujo *et al.* 2020). Finally, we carried out a ground validation of the crown-tag assignments on the field for a random sample of 3% of the total number of trees initially delineated as well as for

trees that were classified as unreliable during the crown delineation process. We calculated ECA (m^2) as the polygon area of each crown-delineated tree.

2.2.6 Total crown area (CA)

We estimated the CA (m^2) of each crown-delineated tree at the time of the RPAS flight based on an allometric model constructed from a crown survey for 622 trees of 148 species in the AFDP. In this crown survey, we measured the DBH and the four radii of the crown of each tree (*sensu* Bohlman & O'Brien 2006). We calculated the crown area based on the averaged radius assuming circular crowns and excluded heavily damaged trees. We fitted a Linear Mixed-Effects Model (LMM) of total crown area as a function of DBH following a power function (i.e., $CA = aDBH^b$), and included species (s) random intercepts and slopes to account for differences in tree architecture (Martínez-Cano *et al.* 2019; Zuleta *et al.* 2022b) (Table S1; Figure S5):

$$\log(CA) = Normal(\mu, \sigma)$$

$$\mu = \beta_{0,s} + \beta_{1,s} \times DBH$$

$$\beta_{0,s} \sim Normal(\beta_0, \sigma_0)$$

$$\beta_{1,s} \sim Normal(\beta_1, \sigma_1)$$

We evaluated the model residuals following a simulation-based approach (Figure S6). The total crown area for each of the crown-delineated trees was obtained from the predictions of this model based on the DBH_{flight} and the species identity. Species-specific random parameters were used if the species was present in the crown survey (78 species), whereas parameters from the averaged-population model were used if the species was not in the crown survey (187 species). We multiplied the model predictions by $\exp(RSE^2/2)$ to correct the bias introduced by back transforming predictions of log-scale models (RSE: residual standard error of the fitted model) (Baskerville, 1972). Species-specific parameters are shown in Table S2.

Author Manuscript

Author Manuscript

2.2.7 Species wood density (WD)

We obtained WD (g cm^{-3}) for each species according to literature (Zanne *et al.* 2009), giving priority to data nearest to the AFDP. When species-level values were not available we used genus-level or family-level averages (Chave *et al.* 2006). Out of the 265 species in our sample, 163, 73, and 26 were assigned the wood density at the species, genus, and family levels, and only three species were assigned the average wood density in the plot (0.60 g cm^{-3}).

2.2.8 Tree mortality rates

For descriptive purposes, we calculated the annual mortality rate (λ, % yr^{-1}) of canopy trees between the date of the RPAS flight and 2019 as:

$$\lambda = \frac{log(N_{flight}) - log(S_{2019})}{time_{2019} - time_{flight}},$$

where N_{flight} is the number of trees alive at $time_{flight}$ (second census) and S_{2019} is the number of those trees that survived until $time_{2019}$ (third census).

Of the 984 canopy trees in our sample, we recorded 101 dead trees (10.3%) after a mean period of 6 (*SD* = 0.2, min = 5.6, max = 6.3) years, which corresponded to an annual mortality rate of 1.82% yr^{-1}. Dead canopy trees were found all over the 18 ha sampled in the AFDP (Figure S7). Trees in our sample covered a wide range of diameters (10.73 – 138.84 cm, DBH), crown areas (21.54 – 473.72 m^2, CA), sun-exposed crown areas (2.45 – 460.87 m^2, ECA), species-adjusted growth rates (-4.19 – 4.25, SA-GR), and species' wood densities (0.20 – 1.05 g cm^{-3}, WD) (Table S3; Figure S8).

2.3 Model fitting

To assess the influence of relative crown exposure to light, species-adjusted tree growth rates, tree size and species wood density on the mortality of canopy trees in the AFDP, we investigated

Author Manuscript

the variables or combination of variables that best explained the probability of death using Generalized Linear Mixed-Effects Models (GLMM, logit link) including species random intercepts. We fitted 16 GLMMs with all possible combinations of covariates and their second-order interactions, including the full (all covariates) and the null (i.e., only intercept) models. We calculated their second-order Akaike's information criterion (AICc) using the *AICcmodavg* package (Mazerolle 2020). We ranked the models and selected the one with the lowest AICc as the best model (Burnham & Anderson 2002). We also considered the inclusion of the log-transformed exposed crown area (log(ECA)) and the modulus-transformed tree growth rate (GR) as covariates but they were removed during preliminary analysis due to their high collinearity with other variables (Table S4).

Mixed-effects models were fitted by maximum likelihood estimation (Laplace approximation) using the *lme4* R package (Bates *et al.* 2015). Model residuals were evaluated with the *simulateResiduals* and *testOutliers* functions of the *DHARMa* R package (Hartig 2021). Conditional (R^2C) and marginal coefficients (R^2M) of determination were calculated with the *MuMIn* R package (Barton 2022). All analyses were performed in R v.4.0.4 (R Core Team 2021).

3. RESULTS

The mortality model with the lowest AICc included RCEL, WD, SA-GR, and their second-order interactions (Tables 1, S5). The main effects of these variables and the interaction between RCEL and WD were highly significant (Table 2). Our model was correctly specified according to residual diagnostics (Figure S9), and there was no evidence of spatial autocorrelation in the

probability of death (Figure S10) or in the residuals of the model (Figure S11). Overall, the probability of death decreased as the WD and the SA-GR increased (Figs. 2a,b).

The main effect of RCEL on the probability of death was constant, both the least sun-exposed trees (RCEL = 0.04) and totally sun-exposed trees (RCEL = 1) had similar probabilities of dying after 6 years (Figure 2c). However, the effect of RCEL was influenced by its interaction with WD and SA-GR (Tables 1, S5). RCEL was negatively related to mortality for trees belonging to species with lower WD (Figure 3a) but tended to be positively related to mortality for trees with higher WD (Figure 3c). The negative effect of SA-GR on the probability of death was stronger for trees with lower WD (Figure 3, S12). Overall, higher probabilities of death were predicted for trees with lower RCEL, lower WD, and lower SA-GR simultaneously.

4. DISCUSSION

We studied the role of crown exposure to light, growth, tree size, and species' wood density on the mortality of canopy trees in the Amacayacu Forest Dynamics Plot (AFDP), northwestern Amazon. While tree mortality relationships with species' wood density and tree growth were mostly confirmatory, an interesting interaction arose between these variables and the proportion of the crown exposed to sunlight. Trees with lower wood density were less prone to die when their proportion of crown was more exposed to sunlight, especially for trees growing less than their species average. On the other hand, trees with higher wood density were slightly more prone to die with higher relative crown exposure. These results highlight the role of wood density in shaping differential survival strategies of canopy trees under varying light conditions.

Author Manuscript

Author Manuscript

Overall, canopy trees of species with lower wood density were more prone to die, a general pattern found across tropical forests (Nascimento *et al.* 2005; Poorter *et al.* 2008; Aleixo *et al.* 2019; Arellano *et al.* 2019; Bauman *et al.* 2022; Reis *et al.* 2022). The higher survival of species with higher wood density is achieved via higher resistance to pathogen attack (Augspurger & Kelly 1984), reduced vulnerability to drought-induced hydraulic failure (Hacke *et al.* 2001; Santiago *et al.* 2018), higher tree mechanical stability (Poorter *et al.* 2008), and less susceptibility to crown damage (Arellano *et al.* 2019). The higher mechanical stability provided by denser wood may be particularly critical for trees in the canopy layer, which are more prone to be disturbed by strong winds and storms and have a higher probability of being directly struck by lightning compared to trees in the understory (Yanoviak *et al.* 2020; Gora & Esquivel-Muelbert 2021).

Trees that grew less than their species average (negative SA-GR) had a higher probability of death than trees that grew more than their species average (positive SA-GR). This pattern was also found by Arellano *et al. (2019)* for trees with DBH≥10 cm in the Lambir forest dynamics plot in tropical Asia, using a similar species-adjusted standardization of individual growth. Other studies have found that trees with low, near-zero growth rates, were more prone to die than trees with higher growth rates (Rüger *et al.* 2011; Camac *et al.* 2018; Esquivel-Muelbert *et al.* 2020). These results support the idea of employing tree growth rates, relative to conspecifics, as a proxy of the health status of individual trees (Chao *et al.* 2009; Bigler *et al.* 2004). Unhealthy trees tend to grow more slowly and have low carbon budgets (Rüger *et al.* 2011; Caac *et al.* 2018), which, in turn, reduces trees' ability to tolerate stress and ultimately survive. The extent to which a slow growth rate is a cause or a consequence of a process killing trees is yet to be determined.

Author Manuscript

The survival of trees with lower wood density depended on both having large proportions of their crowns exposed to vertical sunlight and growing more than their species' average. This result is in line with the expected differential effect of light on the mortality of trees across life-history strategies (light-demanding vs shade-tolerant species) (Nascimento *et al.* 2005; Poorter *et al.* 2008; Wright *et al.* 2010; Rüger *et al.* 2012). The decreasing probability of death for trees with lower wood density with increasing relative crown exposure to light indicates that light-demanding, fast-growing species benefit from being more exposed to sunlight because they require high light conditions to compensate for their higher maintenance costs (Givnish 1988; Lüttge 2008). In addition, this light-dependent survival of trees with lower wood density was particularly pronounced for trees growing less than their species average. Trees with lower wood density, regardless of their species-adjusted growth rate, tended to have lower probabilities of death when their crowns were fully exposed to sunlight. Light-demanding species with low wood density have been shown to have more positive growth responses to light availability compared to species with higher wood density (Rüger *et al.* 2012; Cifuentes & Moreno 2022), which is in line with the sharp decrease in the probability of death with increasing light exposure in trees with lower wood density.

On the contrary, towards the high range of wood densities, we found a slight increase in the probability of death with increasing relative crown exposure to light. A likely explanation for this result could be that shade-tolerant understory species may have experienced abrupt increases in light availability caused by new gap openings, which increased their risk of mortality due to the exposure to photosynthetically active radiation high above the light saturation point, leading to high leaf stress and photoinhibition (Valladares & Niinemets 2008; but see Cifuentes & Moreno 2022). However, most of the dead trees with high wood density were canopy species of

Author Manuscript

terra firme forests in the Northwestern Amazon (e.g., *Eschweilera* genus, *Brosimum guianense*, *Licania micrantha*, *Pouteria hispida*) and are expected to tolerate high exposure to light. Therefore, other unmeasured factors such as droughts (Bennett *et al.* 2015), higher temperatures, lower humidity, higher evaporative demands (Bin *et al.* 2022), and structural damage (Zuleta *et al.* 2022a) are more likely to have contributed to the increase in mortality of trees with higher wood density with increasing exposure to sunlight.

One approach to determining the causes of tree death would have involved gathering post-mortem information by examining the "modes of death". This method, commonly employed to infer mechanisms of tree mortality, attributes dead standing trees to physiological factors and dead broken/uprooted trees to mechanical factors (Gale & Barfod, 1999). However, recent studies have raised concerns about this approach because trees found dead with a specific mode can result from a combination of mechanical and physiological stressors (Zuleta et al. 2022a; Larson and Franklin 2010). For instance, lightning strikes, droughts, and pathogens can all result in groups of standing dead trees presumed to have died by a physiological stressor (Zuleta et al. 2022a; Yanoviak et al., 2020). Similarly, dead broken and uprooted trees, traditionally attributed to mechanical factors (e.g., storms), can actually result from root fungal infections, internal wood rot (Larson and Franklin 2010), or simply be dead standing trees undergoing gradual decomposition. It is important to recognize that the causes of tree death can be more complex and interconnected than traditionally presumed through the modes of death approach (Franklin et al. 1987; Zuleta et al. 2022a).

Although light varies along a continuum across forest strata, the vast majority of studies use a categorical index to characterize the light availability of trees (e.g., crown illumination index; (Clark & Clark 1992), adapted from Dawkins & Field (1978)). We used a continuous

Author Manuscript

metric for light availability that accounts for the proportion of total tree crown area that is exposed to vertical sunlight (i.e., RCEL) and reflects the amount of resources allocated to the crown that are potentially intercepting direct light. Given that the crown holds the machinery for capturing and transforming light into resources for growth and tree maintenance, RCEL could also be interpreted as a proxy for tree vigor. An RCEL value lower than one indicates that a portion of the crown area is not observed from above, which may be influenced by at least two non-mutually exclusive mechanisms: crown shading and crown damage. Synchronized ground-based assessments of tree damage and RPAS-based assessments of tree crowns would be needed to disentangle these mechanisms.

Since crown area is inherently correlated to tree diameter, an obvious question is if RCEL relates to DBH and to what extent are these variables related to tree survival. In our modeling results, the second model with the lowest AICc included DBH instead of RCEL (Tables 1, S5) and predictions of probability of death based on the model with DBH were similar to predictions from the model including RCEL (Figure S13). However, the correlation between RCEL and log(DBH) was low (Figure S14; Pearson's correlation coefficient = -0.0790, $P<0.05$), indicating that both individual-level variables may reflect different mechanisms. While RCEL is associated with the actual exposure of the tree to direct light (as discussed above), DBH is primarily a metric for trunk size. Deviations between RCEL and DBH may be due to tree architecture, crown plasticity, tree light competition, forest gaps, and tree damage (Jucker *et al.* 2015; Zuleta *et al.* 2022b). For example, a tree with 10 cm of DBH can be either fully exposed to light, shaded by other trees, or highly damaged. This is very likely the reason why the best model explaining tree survival of canopy trees in our study included RCEL instead of DBH. It is worth noting,

however, that RCEL does not capture the full spectrum of tree light interception along the vertical forest strata (Lüttge 2008; Bin *et al.* 2022).

5. Conclusion

Our results highlight the importance of the inclusion of plant functional types related to life history strategies (e.g., proxied by wood density) in vegetation dynamic models aiming to predict forest demography under ongoing global changes. Moreover, our study demonstrates how the integration of high-resolution remote sensing with ground-based data can be used to better quantify tree-level factors associated with tree mortality. The fast development and increasing accessibility of remote sensing products constitute a promising tool to better understand the influence of climatic drivers (e.g., increasing vapor pressure deficit, high winds) on tree mortality as well as the individual- and species-level factors that mediate these responses (e.g., RCEL) at large spatial scales (Cushman *et al.* 2022; McDowell *et al.* 2022).

Author Manuscript

Author Manuscript

TABLES

Table 1. Comparison of GLMMs employed to predict canopy tree mortality (M) using individual- and species-level factors. Models are ranked according to the difference in Akaike information criterion value corrected for small samples (ΔAICc) compared to the best model. Nested models with higher ΔAICc are removed from the table and presented in Table S5 for presentation purposes. Candidate fixed effects were relative crown exposure to light (RCEL, unitless), log-transformed size (log(DBH), cm), wood density (WD, g cm^{-3}) and species-adjusted growth rate (SA-GR, unitless). All models included species as random intercept and second-order interactions among the fixed effects. Marginal (R^2M) and conditional (R^2C) R^2 are the amount of variation explained by fixed effects and combined fixed + random effects, respectively (Nakagawa & Schielzeth, 2013). Total number of parameters (K), root mean squared error (RMSE) and log-likelihood (LL) are given for each model.

Model	K	R^2M	R^2C	RMSE	LL	AICc	ΔAICc
M ~ RCEL + WD + SA-GR + RCEL*WD + RCEL*SA-GR + WD*SA-GR	8	0.06	0.23	0.28	-307.61	631.38	0.00
M ~ WD + log(DBH) + SA-GR + WD*log(DBH) + WD*SA-GR + log(DBH)*SA-GR	8	0.07	0.21	0.28	-308.67	633.50	2.12
M ~ RCEL + WD + log(DBH) + SA-GR + RCEL*WD + RCEL*log(DBH) + RCEL*SA-GR + WD*log(DBH) + WD*SA-GR + log(DBH)*SA-GR (full model)	12	0.09	0.26	0.28	-304.86	634.04	2.67
M ~ 1 (null model)	2	0.00	0.17	0.29	-319.51	643.03	11.65

Author Manuscript

Table 2. Parameter estimates and statistics for the generalized linear mixed-effects canopy tree mortality model with the lowest AICc in the Amacayacu Forest Dynamics Plot, northwestern Amazon. Relative crown exposure to light (RCEL, unitless), wood density (WD, g cm^{-3}), and species-adjusted growth rate (SA-GR, unitless). CI: confidence interval of the estimate. σ^2: residual variance. T_{00}: variance of the species random intercept. ICC: interclass correlation coefficient.

Predictors	***Log-Odds***	***CI***	***p***
(Intercept)	1.60	-0.37 – 3.58	0.112
RCEL	-5.13	-8.76 – -1.50	**0.006**
WD	-5.86	-9.23 – -2.49	**0.001**
SA-GR	-1.19	-2.18 – -0.20	**0.019**
RCEL * WD	7.36	1.41 – 13.31	**0.015**
RCEL * SA-GR	0.66	-0.08 – 1.40	0.079
WD * SA-GR	1.05	-0.46 – 2.55	0.174
Random Effects			
σ^2	3.29		
$\tau_{00\ species}$	0.73		
ICC	0.18		
$N_{\ species}$	265		
Observations	984		
Marginal R^2 / Conditional R^2	0.062 / 0.232		

Author Manuscript

Author Manuscript

FIGURE LEGENDS

Figure 1. Outline of methodology to estimate the Relative Crown Exposure to Light (RCEL) of canopy trees in the Amacayacu Forest Dynamics Plot (AFDP), northwestern Amazon. (a) The vertically sun-Exposed Crown Area (ECA, green polygons) of 984 trees of 265 species (48 families) was estimated using a near-infrared orthomosaic of the canopy of the AFDP. (b) Detailed ECA delineation with the corresponding tree tag. (c) Ground-based Crown Area (CA) survey for 622 trees of 148 species at the AFDP, where the DBH and four radii of the crown of each tree were measured. (d) The CA survey was used to construct a Linear Mixed-Effects Model (LMM) to predict total CA as a function of DBH following a power function with species random intercepts and slopes. (e) Representation of the vertically sun-exposed crown area (ECA) and the total crown area (CA) to estimate (f) the relative crown exposure to light (RCEL) of a given tree. In (a) and (b) green polygons correspond to the vertically sun-exposed crown boundaries of each tree (i.e., observed from above) and black lines indicate 20 m x 20 m quadrats. This study was restricted to 18 out of 25 ha for which the survival of trees were assessed prior to the COVID-19 Pandemic. Figure S7 shows the status of these canopy trees (alive or dead) in 2019.

Figure 2. Predicted probability of death (%) for canopy trees in the AFDP as a function of (a) wood density (WD, g cm^{-3}), (b) species-adjusted growth rate (SA-GR, unitless), and (c) relative crown exposure to light (RCEL, unitless). Lines represent the adjusted predictions from the model for each variable leaving the others conditioned at their mean and shaded areas indicate the 95% confidence interval. Point sizes are scaled according to the DBH of the trees. The second vertical axis, λ, shows the corresponding annual mortality rate (% yr^{-1}) for the predicted

probability of death in a 6-year period. The color of the points in (b) and (c) indicates WD classes defined based on the average wood density ± 1 SD of all trees ≥ 10 cm DBH in the plot.

Figure 3. Predicted probability of death (%) for canopy trees in the AFDP as a function of relative crown exposure to light (RCEL, unitless) for three classes of wood density (WD, panels) within three classes of species-adjusted growth rate (SA-GR, color points). Lines represent the adjusted predictions from the model conditioned to reference values and shaded areas indicate the 95% confidence interval. Point sizes are scaled according to the DBH of the trees. The second vertical axis, λ, shows the corresponding annual mortality rate (% yr^{-1}) for the predicted probability of death in a 6-year period. Reference values were adjusted for WD at 0.41 g cm^{-3} in (a), 0.60 g cm^{-3} in (b) and 0.83 g cm^{-3} in (c), which correspond to the average wood density ± 1 SD of all trees ≥ 10 cm DBH in the plot. Reference values were adjusted for SA-GR at: -0.90 for trees with SA-GR ≤ 0 (green points), 1.03 for trees with 0 < SA-GR ≤ 2 (orange points), and 2.51 for trees with SA-GR > 2 (purple points).

Author Manuscript

Author Manuscript

FIGURES

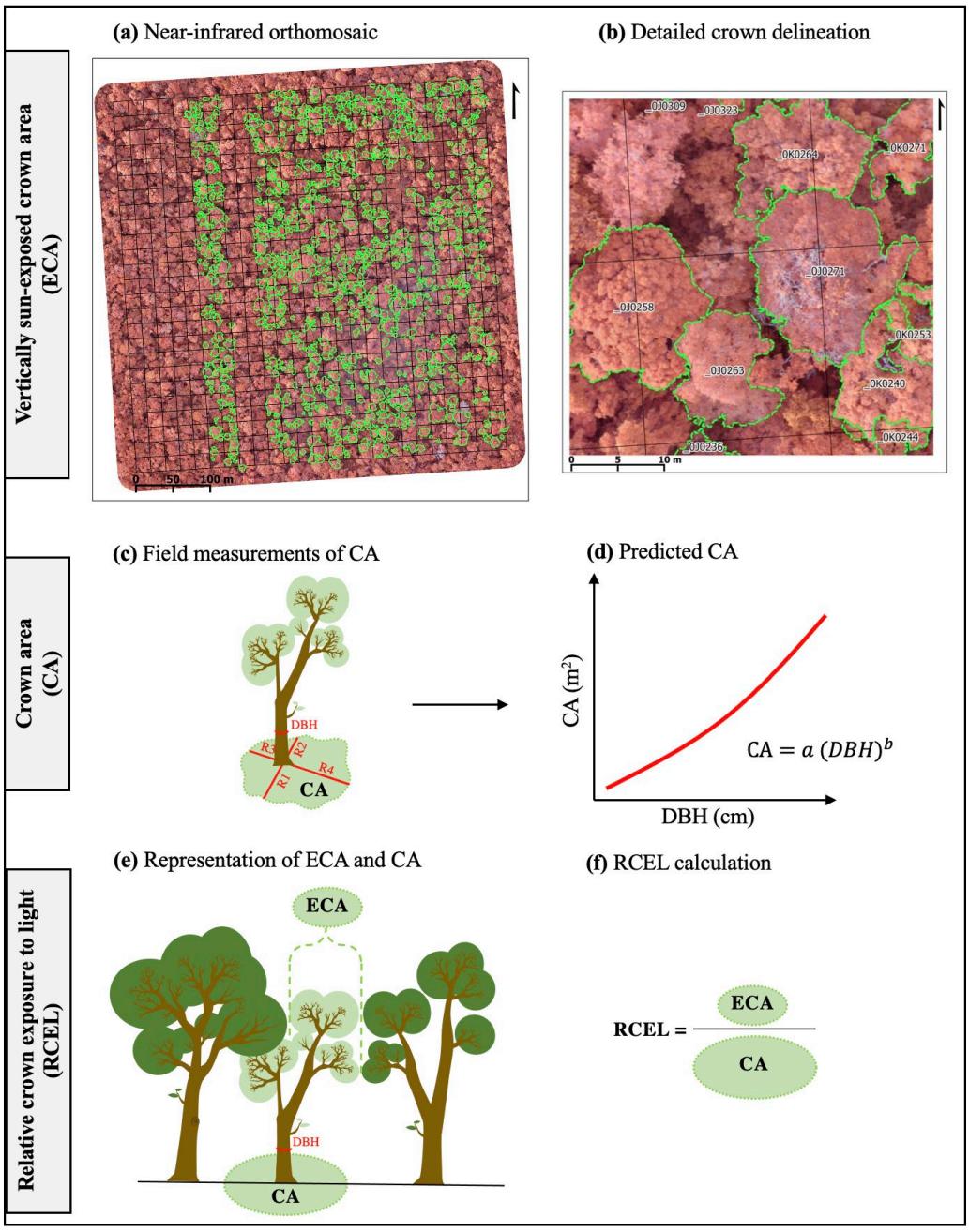

Figure 1. Outline of methodology to estimate the Relative Crown Exposure to Light (RCEL) of canopy trees in the Amacayacu Forest Dynamics Plot (AFDP), northwestern Amazon. (a) The vertically sun-Exposed Crown Area (ECA, green polygons) of 984 trees of 265 species (48 families) was estimated using a near-infrared orthomosaic of the canopy of the AFDP. (b)

Detailed ECA delineation with the corresponding tree tag. (c) Ground-based Crown Area (CA) survey for 622 trees of 148 species at the AFDP, where the DBH and four radii of the crown of each tree were measured. (d) The CA survey was used to construct a Linear Mixed-Effects Model (LMM) to predict total CA as a function of DBH following a power function with species random intercepts and slopes. (e) Representation of the vertically sun-exposed crown area (ECA) and the total crown area (CA) to estimate (f) the relative crown exposure to light (RCEL) of a given tree. In (a) and (b) green polygons correspond to the vertically sun-exposed crown boundaries of each tree (i.e., observed from above) and black lines indicate 20 m x 20 m quadrats. This study was restricted to 18 out of 25 ha for which the survival of trees were assessed prior to the COVID-19 Pandemic. Figure S7 shows the status of these canopy trees (alive or dead) in 2019.

Author Manuscript

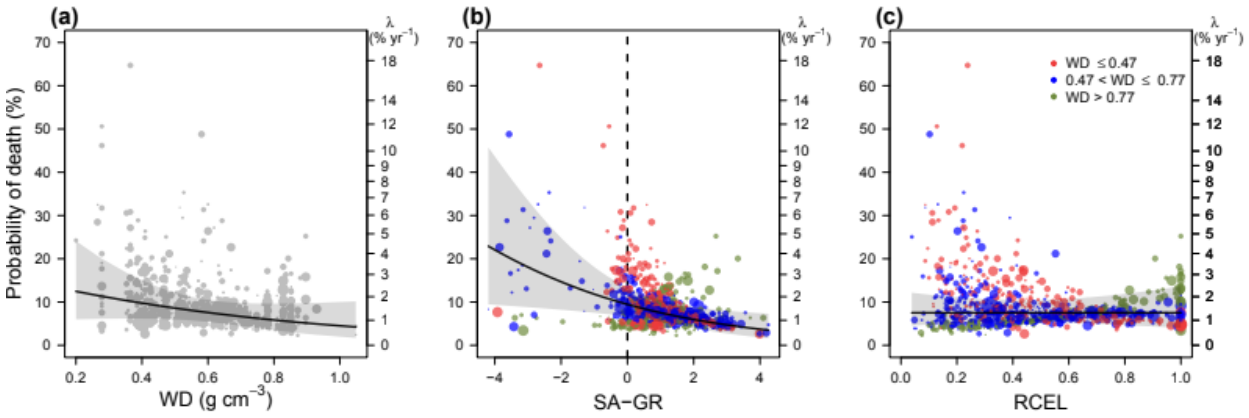

Figure 2. Predicted probability of death (%) for canopy trees in the AFDP as a function of (a) wood density (WD, g cm^{-3}), (b) species-adjusted growth rate (SA-GR, unitless), and (c) relative crown exposure to light (RCEL, unitless). Lines represent the adjusted predictions from the model for each variable leaving the others conditioned at their mean and shaded areas indicate the 95% confidence interval. Point sizes are scaled according to the DBH of the trees. The second vertical axis, λ, shows the corresponding annual mortality rate (% yr^{-1}) for the predicted probability of death in a 6-year period. The color of the points in (b) and (c) indicates WD classes defined based on the average wood density ± 1 SD of all trees ≥ 10 cm DBH in the plot.

Author Manuscript

Author Manuscript

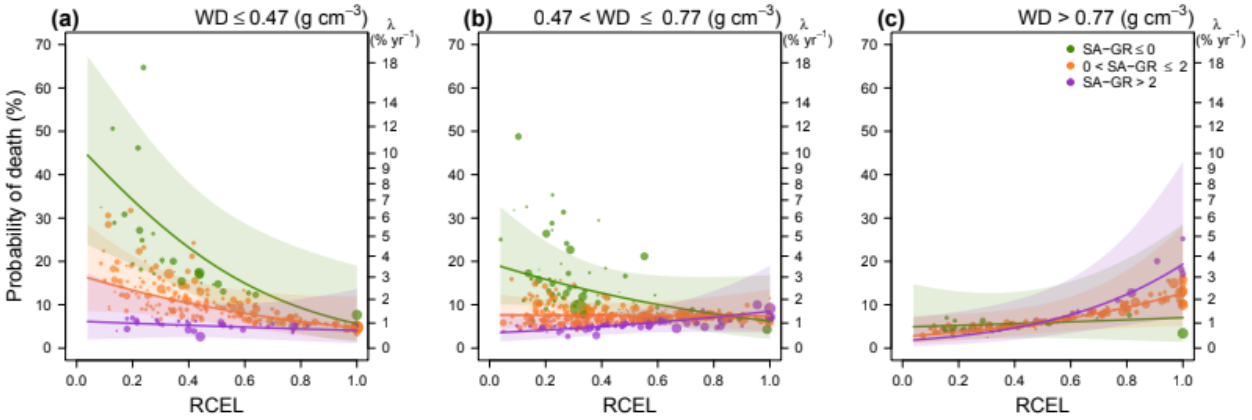

Figure 3. Predicted probability of death (%) for canopy trees in the AFDP as a function of relative crown exposure to light (RCEL, unitless) for three classes of wood density (WD, panels) within three classes of species-adjusted growth rate (SA-GR, color points). Lines represent the adjusted predictions from the model conditioned to reference values and shaded areas indicate the 95% confidence interval. Point sizes are scaled according to the DBH of the trees. The second vertical axis, λ, shows the corresponding annual mortality rate (% yr^{-1}) for the predicted probability of death in a 6-year period. Reference values were adjusted for WD at 0.41 g cm^{-3} in (a), 0.60 g cm^{-3} in (b) and 0.83 g cm^{-3} in (c), which correspond to the average wood density ± 1 SD of all trees ≥ 10 cm DBH in the plot. Reference values were adjusted for SA-GR at: -0.90 for trees with SA-GR ≤ 0 (green points), 1.03 for trees with 0 < SA-GR ≤ 2 (orange points), and 2.51 for trees with SA-GR > 2 (purple points).

Author Manuscript

ACKNOWLEDGEMENTS

LFG-C and CJ-H were supported by MinCiencias "Convocatoria 891 2020". DZ was supported as part of the NGEE-T, funded by the US Department of Energy, Office of Science, Office of Biological and Environmental Research (https://ngee-tropics.lbl.gov/). Ground-based data collection was supported by the ForestGEO of the Smithsonian Institution. The NIR images were collected during the 9th Regional SilvaCarbon/GFOI Workshop on Forest Monitoring. This project was possible thanks to the commitment of Dr. Dairon Cárdenas (1957–2022), E. Martínez, S. Sua, A. Barona, and coworkers from the Palmeras Indigenous Community as well as the administrative crew at SINCHI and Parques Nacionales Naturales de Colombia. We thank M. Gutiérrez, S. Múnera, and hundreds of technicians and students of forest engineering at Universidad Nacional de Colombia that have worked on data collection and cleaning.

AUTHOR CONTRIBUTION STATEMENT

DZ and LFG-C conceptualized the study. LFG-C, CJ-H, and DZ performed formal analysis, and contributed to methodology, software, validation and visualization. LFG-C, CJ-H, NC, DZ, RFA, GA, JH, AD, and FE performed data curation. AD, NC, and SJD contributed to funding acquisition and provided resources. DZ and AD performed supervision. LFG-C and DZ wrote the original draft. All authors wrote, reviewed and edited the manuscript.

DATA AVAILABILITY STATEMENT

The data that support the findings of this study are openly available in the NGEE Tropics Data Collection at http://doi.org/10.15486/ngt/1993900 (Gómez-Correa et al. 2023).

DISCLOSURE STATEMENTS

The corresponding author confirms on behalf of all authors that there have been no involvements that might raise the question of bias in the work reported or in the conclusions, implications, or opinions stated.

Author Manuscript

Author Manuscript

REFERENCES

Aleixo, I., Norris, D., Hemerik, L., Barbosa, A., Prata, E., Costa, F., *et al.* (2019). Amazonian rainforest tree mortality driven by climate and functional traits. *Nat. Clim. Chang.*, 9, 384–388.

Araujo, R.F., Chambers, J.Q., Celes, C.H.S., Muller-Landau, H.C., Santos, A.P.F. dos, Emmert, F., *et al.* (2020). Integrating high resolution drone imagery and forest inventory to distinguish canopy and understory trees and quantify their contributions to forest structure and dynamics. *PLoS One*, 15, e0243079.

Arellano, G., Medina, N.G., Tan, S., Mohamad, M. & Davies, S.J. (2019). Crown damage and the mortality of tropical trees. *New Phytol.*, 221, 169–179.

Augspurger, C.K. & Kelly, C.K. (1984). Pathogen mortality of tropical tree seedlings: experimental studies of the effects of dispersal distance, seedling density, and light conditions. *Oecologia*, 61, 211–217.

Barton, K. (2022). MuMIn: Multi-Model Inference.

Baskerville, G.L. (1972). Use of logarithmic regression in the estimation of plant biomass. *Canadian Journal of Forest Research*, 2(1), 49-53.

Bates, D., Mächler, M., Bolker, B. & Walker, S. (2015). Fitting Linear Mixed-Effects Models Using lme4. *J. Stat. Softw.*, 67, 1–48.

Bauman, D., Fortunel, C., Delhaye, G., Malhi, Y., Cernusak, L.A., Bentley, L.P., *et al.* (2022a). Tropical tree mortality has increased with rising atmospheric water stress. *Nature*.

Bennett, A.C., McDowell, N.G., Allen, C.D. & Anderson-Teixeira, K.J. (2015). Larger trees suffer most during drought in forests worldwide. *Nat. Plants*, 1, 15139.

Author Manuscript

Bin, Y., Li, Y., Russo, S.E., Cao, H., Ni, Y., Ye, W., *et al.* (2022). Leaf trait expression varies with tree size and ecological strategy in a subtropical forest. *Funct. Ecol.*, 36, 1010–1022.

Bigler, C., Gričar, J., Bugmann, H., & Čufar, K. (2004). Growth patterns as indicators of impending tree death in silver fir. *For. Ecol. and Manag.,* 199(2-3), 183-190.

Bohlman, S.A. & O'Brien, S. (2006). Allometry, adult stature and regeneration requirement of 65 tree species on Barro Colorado Island, Panama. *J. Trop. Ecol.*, 22, 123–136.

Burnham, K.P. & Anderson, D.R. (2002). *Model selection and multi- model inference. A practical information-theoretic approach*. 2nd edn. Springer New York, NY, New York, NY.

Camac, J.S., Condit, R., FitzJohn, R.G., McCalman, L., Steinberg, D., Westoby, M., *et al.* (2018). Partitioning mortality into growth-dependent and growth-independent hazards across 203 tropical tree species. *Proc. Natl. Acad. Sci.*, 115, 12459–12464.

Chamorro, C. (1989). Biología de los suelos del Parque Nacional Natural Amacayacu y zonas adyacentes (Amazonas, Colombia). *Colomb. Geográfica*, 15, 45–63.

Chao, K. J., Phillips, O. L., Monteagudo, A., Torres-Lezama, A. & Martinez, R. V. How do trees die? Mode of death in northern Amazonia. *J. Veg. Sci.* 20, 260–268 (2009).

Chave, J., Coomes, D., Jansen, S., Lewis, S.L., Swenson, N.G. & Zanne, A.E. (2009). Towards a worldwide wood economics spectrum. *Ecol. Lett.*, 12, 351–366.

Chave, J., Muller-Landau, H.C., Baker, T.R., Easdale, T.A., ter Steege, H. & Webb, C.O. (2006). Regional and phylogenetic variation of wood density across 2456 neotropical tree species. *Ecol. Appl.*, 16, 2356–2367.

Cifuentes, L. & Moreno, F. (2022). Trait coordination at leaf level explains the resistance to excess light stress in shade-tolerant tropical tree species. *Tree Physiol.*, 42, 1325–1336.

Author Manuscript

Clark, D.A. & Clark, D.B. (1992). Life History Diversity of Canopy and Emergent Trees in a Neotropical Rain Forest. *Ecol. Monogr.*, 62, 315–344.

Condit, R., Aguilar, S., Hernandez, A., Perez, R., Lao, S., Angehr, G., *et al.* (2004). Tropical forest dynamics across a rainfall gradient and the impact of an El Niño dry season. *J. Trop. Ecol.*, 20, 51–72.

Condit, R., Pérez, R., Lao, S., Aguilar, S. & Hubbell, S.P. (2017). Demographic trends and climate over 35 years in the Barro Colorado 50 ha plot. *For. Ecosyst.*, 4, 17.

Cushman, K.C., Bunyavejchewin, S., Cárdenas, D., Condit, R., Davies, S.J., Duque, Á., *et al.* (2021). Variation in trunk taper of buttressed trees within and among five lowland tropical forests. *Biotropica*, 53, 1442–1453.

Cushman, K.C., Detto, M., García, M. & Muller-Landau, H.C. (2022). Soils and topography control natural disturbance rates and thereby forest structure in a lowland tropical landscape. *Ecol. Lett.*, 25, 1126–1138.

Davies, S.J., Abiem, I., Abu Salim, K., Aguilar, S., Allen, D., Alonso, A., *et al.* (2021). ForestGEO: Understanding forest diversity and dynamics through a global observatory network. *Biol. Conserv.*, 253, 108907.

Dawkins, H.C. & Field, D.R.B. (1978). *A long-term surveillance system for british woodland vegetation*. C.F.I. occasional papers. Department of Forestry, Oxford University, Oxford, United Kingdom.

Duque, A., Muller-Landau, H.C., Valencia, R., Cardenas, D., Davies, S.J., de Oliveira, A., *et al.* (2017). Insights into regional patterns of Amazonian forest structure, diversity, and dominance from three large terra-firme forest dynamics plots. *Biodivers. Conserv.*, 26, 669–686.

Author Manuscript

Esquivel-Muelbert, A., Phillips, O.L., Brienen, R.J.W., Fauset, S., Sullivan, M.J.P., Baker, T.R., *et al.* (2020). Tree mode of death and mortality risk factors across Amazon forests. *Nat. Commun.*, 11, 5515.

Feeley, K.J. & Zuleta, D. (2022). Changing forests under climate change. *Nat. Plants* 8, 984–985

Franklin, J.F., Shugart, H.H. & Harmon, M.E. (1987). Tree death as an ecological process. *Bioscience*, 37, 550–556.

Friedlingstein, P., Jones, M.W., O'Sullivan, M., Andrew, R.M., Bakker, D.C.E., Hauck, J., *et al.* (2022). Global Carbon Budget 2021. *Earth Syst. Sci. Data*, 14, 1917–2005.

Gale N., Barfod A.S. (1999). Canopy tree mode of death in a western Ecuadorian rain forest. *Journal of Tropical Ecology*, 15, 415–436.

Givnish, T. (1988). Adaptation to sun and shade: a whole-plant perspective. *Funct. Plant Biol.*, 15, 63.

Gómez-Correa, L., Duque, A., Castaño, N., Haarpaintner, J., Enßle, F., Jaramillo-Hernández, C., Zuleta, D. (2023). Canopy tree mortality and crown exposure data from the Amacayacu Forest Dynamics Plot, Northwestern Amazon. 1.0. NGEE Tropics Data Collection. (dataset). https://doi.org/10.15486/ngt/1993900

Gora, E.M. & Esquivel-Muelbert, A. (2021). Implications of size-dependent tree mortality for tropical forest carbon dynamics. *Nat. Plants*, 7, 384–391.

Grizonnet, M., Michel, J., Poughon, V., Inglada, J., Savinaud, M. & Cresson, R. (2017). Orfeo ToolBox: open source processing of remote sensing images. *Open Geospatial Data, Softw. Stand.*, 2, 15.

Author Manuscript

Hacke, U.G., Sperry, J.S., Pockman, W.T., Davis, S.D. & McCulloh, K.A. (2001). Trends in wood density and structure are linked to prevention of xylem implosion by negative pressure. *Oecologia*, 126, 457–461.

Harris, R.M.B., Beaumont, L.J., Vance, T.R., Tozer, C.R., Remenyi, T.A., Perkins-Kirkpatrick, S.E., *et al.* (2018). Biological responses to the press and pulse of climate trends and extreme events. *Nat. Clim. Chang.*, 8, 579–587.

Hartig, F. (2021). DHARMa: residual diagnostics for hierarchical (multi-level/mixed) regression models.

Heijink, B.M., McMichael, C.N.H., Piperno, D.R., Duivenvoorden, J.F., Cárdenas, D. & Duque, Á. (2020). Holocene increases in palm abundances in north-western Amazonia. *J. Biogeogr.*, 47, 698–711.

Herwitz, S.R., Slye, R.E. & Turton, S.M. (2000). Long-term survivorship and crown area dynamics of tropical rainforest canopy trees. *Ecology*, 81, 585–597.

Hubau, W., Lewis, S.L., Phillips, O.L., Affum-Baffoe, K., Beeckman, H., Cuní-Sanchez, A., *et al.* (2020). Asynchronous carbon sink saturation in African and Amazonian tropical forests. *Nature*, 579, 80–87.

Jucker, T., Bouriaud, O. & Coomes, D.A. (2015). Crown plasticity enables trees to optimize canopy packing in mixed-species forests. *Funct. Ecol.*, 29, 1078–1086.

King, D.A., Davies, S.J. & Noor, N.S.M. (2006). Growth and mortality are related to adult tree size in a Malaysian mixed dipterocarp forest. *For. Ecol. Manage.*, 223, 152–158.

Kobe, R. K., Pacala, S. W., Silander, J. A. & Canham, C. D (1995). Juvenile tree survivorship as a component of shade tolerance. *Ecol. Appl.* 5, 517–532.

Author Manuscript

Larson, A.J., Franklin, J.F. (2010). The tree mortality regime in temperate old-growth coniferous forests: the role of physical damage. *Canadian Journal of Forest Research,* 40, 2091–2103.

Lüttge, U. (2008). Tropical Forests. I. Physiognomy and Functional Structure. In: *Physiological Ecology of Tropical Plants* (ed. Lüttge, U.). Springer Berlin Heidelberg, Berlin, Heidelberg, pp. 51–101.

Lutz, J.A., Furniss, T.J., Johnson, D.J., Davies, S.J., Allen, D., Alonso, A., *et al.* (2018). Global importance of large-diameter trees. *Glob. Ecol. Biogeogr.*, 27, 849–864.

Martínez-Cano, I., Muller-Landau, H.C., Joseph Wright, S., Bohlman, S.A. & Pacala, S.W. (2019). Tropical tree height and crown allometries for the Barro Colorado Nature Monument, Panama: A comparison of alternative hierarchical models incorporating interspecific variation in relation to life history traits. *Biogeosciences*, 16, 847–862.

Mazerolle, M. (2020). AICcmodavg: Model selection and multimodel inference based on (Q)AIC(c).

McDowell, N.G., Sapes, G., Pivovaroff, A., Adams, H.D., Allen, C.D., Anderegg, W.R.L., *et al.* (2022). Mechanisms of woody-plant mortality under rising drought, CO2 and vapour pressure deficit. *Nat. Rev. Earth Environ.*, 3, 294–308.

McMahon, S.M., Arellano, G. & Davies, S.J. (2019). The importance and challenges of detecting changes in forest mortality rates. *Ecosphere*, 10, e02615.

Metcalf, C.J.E., Horvitz, C.C., Tuljapurkar, S. & Clark, D.A. (2009). A time to grow and a time to die: a new way to analyze the dynamics of size, light, age, and death of tropical trees. *Ecology*, 90, 2766–2778.

Muller-Landau, H.C., Condit, R.S., Chave, J., Thomas, S.C., Bohlman, S.A., Bunyavejchewin, S., *et al.* (2006). Testing metabolic ecology theory for allometric scaling of tree size, growth and mortality in tropical forests. *Ecol. Lett.*, 9, 575–588.

Nakagawa, S. & Schielzeth, H. (2013). A general and simple method for obtaining R2 from generalized linear mixed-effects models. *Methods Ecol. Evol.*, 4, 133–142.

Nascimento, H.E.M., Laurance, W.F., Condit, R., Laurance, S.G., D'Angelo, S. & Andrade, A.C. (2005). Demographic and life-history correlates for Amazonian trees. *J. Veg. Sci.*, 16, 625–634.

Negrón-Juárez, R., Jenkins, H., Raupp, C., Riley, W., Kueppers, L., Magnabosco Marra, D., *et al.* (2017). Windthrow variability in Central Amazonia. *Atmosphere (Basel).*, 8, 28.

Piponiot, C., Anderson-Teixeira, K.J., Davies, S.J., Allen, D., Bourg, N.A., Burslem, D.F.R.P., *et al.* (2022). Distribution of biomass dynamics in relation to tree size in forests across the world. *New Phytol.*, 234, 1664–1677.

Poorter, L., Wright, S.J., Paz, H., Ackerly, D.D., Condit, R., Ibarra-Manríquez, G., *et al.* (2008). Are functional traits good predictors of demographic rates? Evidence from five neotropical forests. *Ecology*, 89, 1908–1920.

QGIS Geographic Information System. (2022). QGIS.

R Core Team. (2021). R: a language and environment for statistical computing.

Reich, P. B. (2014). The world- wide 'fast–slow' plant economics spectrum: a traits manifesto. J. Ecol. 102, 275–301.

Reis, S.M., Marimon, B.S., Esquivel-Muelbert, A., Marimon, B.H., Morandi, P.S., Elias, F., *et al.* (2022). Climate and crown damage drive tree mortality in southern Amazonian edge forests. *J. Ecol.*, 110, 876–888.

Author Manuscript

Author Manuscript

Rüger, N., Huth, A., Hubbell, S.P. & Condit, R. (2011). Determinants of mortality across a tropical lowland rainforest community. *Oikos*, 120, 1047–1056.

Rüger, N., Wirth, C., Wright, S.J. & Condit, R. (2012). Functional traits explain light and size response of growth rates in tropical tree species. *Ecology*, 93, 2626–2636.

Russo, S.E., Davies, S.J., King, D.A. & Tan, S. (2005). Soil-related performance variation and distributions of tree species in a Bornean rain forest. *J. Ecol.*, 93, 879–889.

Russo, S.E., McMahon, S.M., Detto, M., Ledder, G., Wright, S.J., Condit, R.S., *et al.* (2021). The interspecific growth–mortality trade-off is not a general framework for tropical forest community structure. *Nat. Ecol. Evol.*, 5, 174–183.

Santiago, L.S., De Guzman, M.E., Baraloto, C., Vogenberg, J.E., Brodie, M., Hérault, B., *et al.* (2018). Coordination and trade-offs among hydraulic safety, efficiency and drought avoidance traits in Amazonian rainforest canopy tree species. *New Phytol.*, 218, 1015–1024.

Valladares, F. & Niinemets, Ü. (2008). Shade Tolerance, a Key Plant Feature of Complex Nature and Consequences. *Annu. Rev. Ecol. Evol. Syst.*, 39, 237–257.

Wright, S.J. (2002). Plant diversity in tropical forests: A review of mechanisms of species coexistence. *Oecologia*, 130, 1–14.

Wright, S.J., Kitajima, K., Kraft, N.J.B., Reich, P.B., Wright, I.J., Bunker, D.E., *et al.* (2010). Functional traits and the growth–mortality trade-off in tropical trees. *Ecology*, 91, 3664–3674.

Yanoviak, S.P., Gora, E.M., Bitzer, P.M., Burchfield, J.C., Muller-Landau, H.C., Detto, M., *et al.* (2020). Lightning is a major cause of large tree mortality in a lowland neotropical forest. *New Phytol.*, 225, 1936–1944.

Zanne, A.E., López-González, G., Coomes, D.A., Ilic, J., Jansen, S., Lewis, S.L., *et al.* (2009). Global wood density database. *Dryad Digit. Repos.*

Zuleta, D., Arellano, G., Muller-Landau, H.C., McMahon, S.M., Aguilar, S., Bunyavejchewin, S., *et al.* (2022a). Individual tree damage dominates mortality risk factors across six tropical forests. *New Phytol.*, 233, 705–721.

Zuleta, D., Duque, A., Cardenas, D., Muller-Landau, H.C. & Davies, S.J. (2017). Drought-induced mortality patterns and rapid biomass recovery in a terra firme forest in the Colombian Amazon. *Ecology*, 98, 2538–2546.

Zuleta, D., Krishna Moorthy, S.M., Arellano, G., Verbeeck, H. & Davies, S.J. (2022b). Vertical distribution of trunk and crown volume in tropical trees. *For. Ecol. Manage.*, 508, 120056.

Zuleta, D., Russo, S.E., Barona, A., Barreto-Silva, J.S., Cardenas, D., Castaño, N., *et al.* (2020). Importance of topography for tree species habitat distributions in a terra firme forest in the Colombian Amazon. *Plant Soil*, 450, 133–149.

Author Manuscript

Author Manuscript

Vertically sun-exposed crown area (ECA)

Crown area (CA)

Relative crown exposure to light (RCEL)

(a) Near-infrared orthomosaic

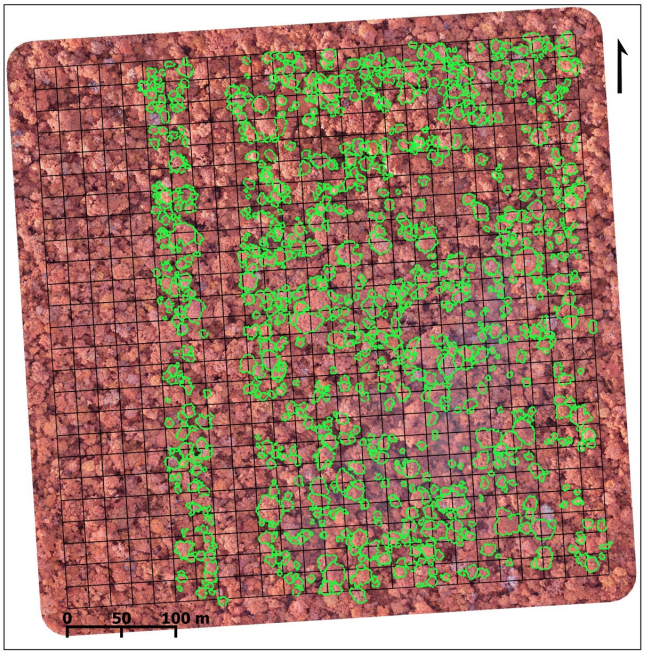

(b) Detailed crown delineation

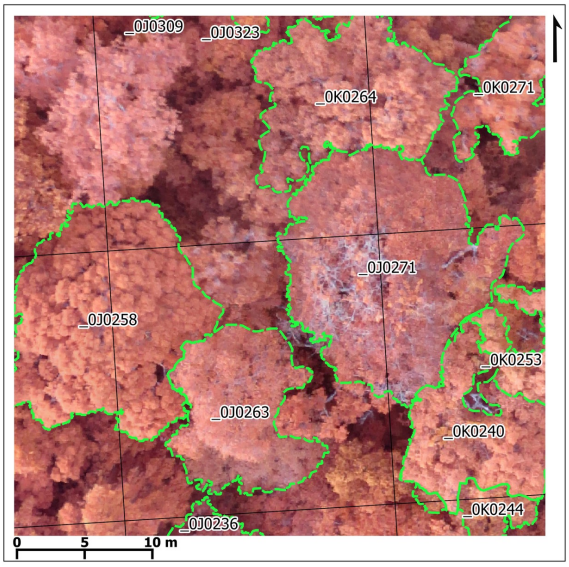

(c) Field measurements of CA

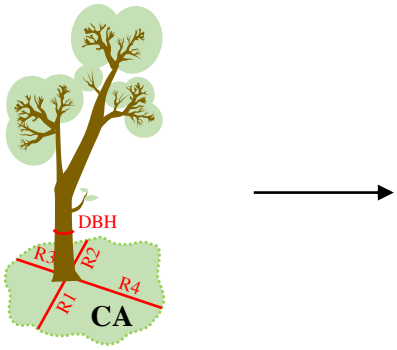

(d) Predicted CA

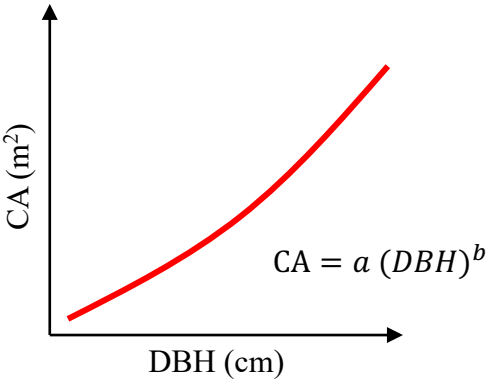

(e) Representation of ECA and CA

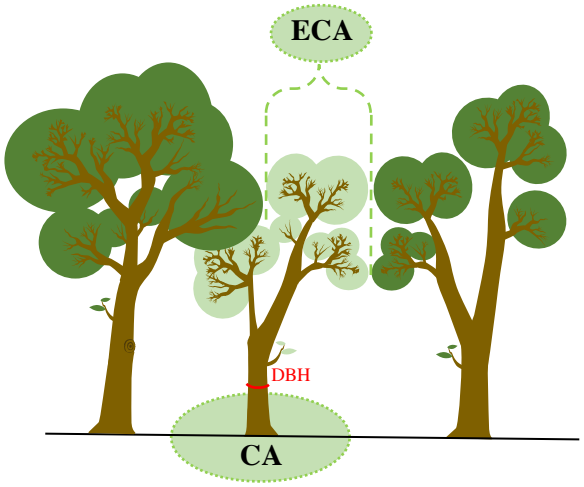

(f) RCEL calculation

$$\text{RCEL} = \frac{\text{ECA}}{\text{CA}}$$

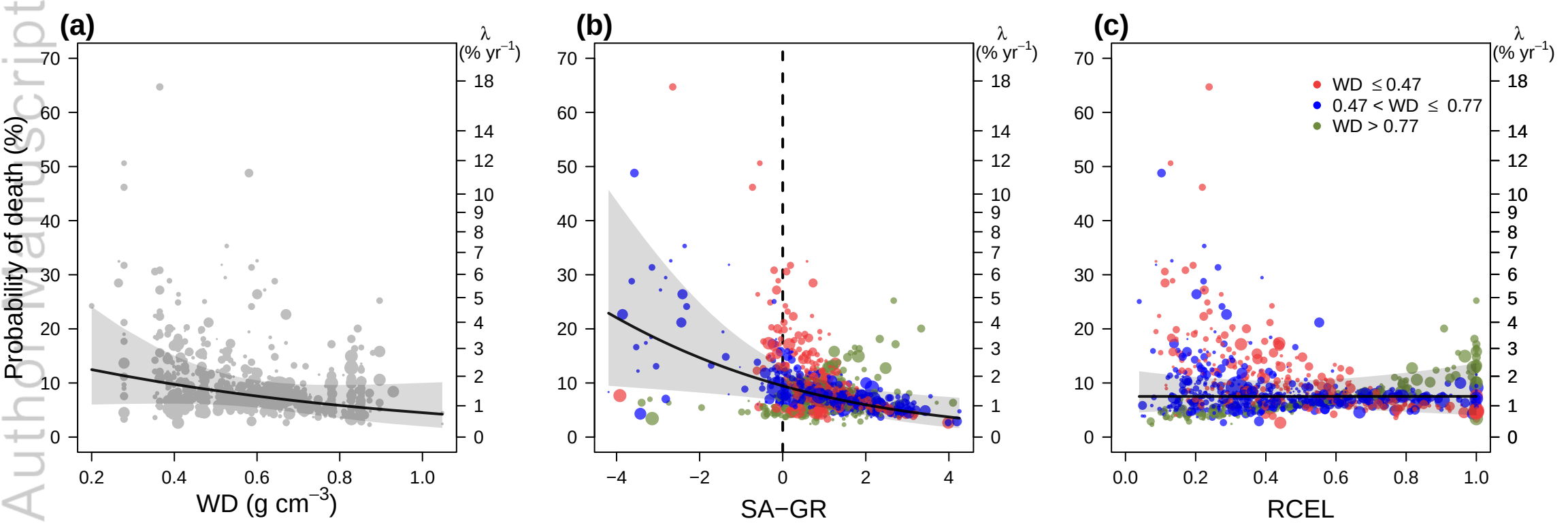

Author Manuscript

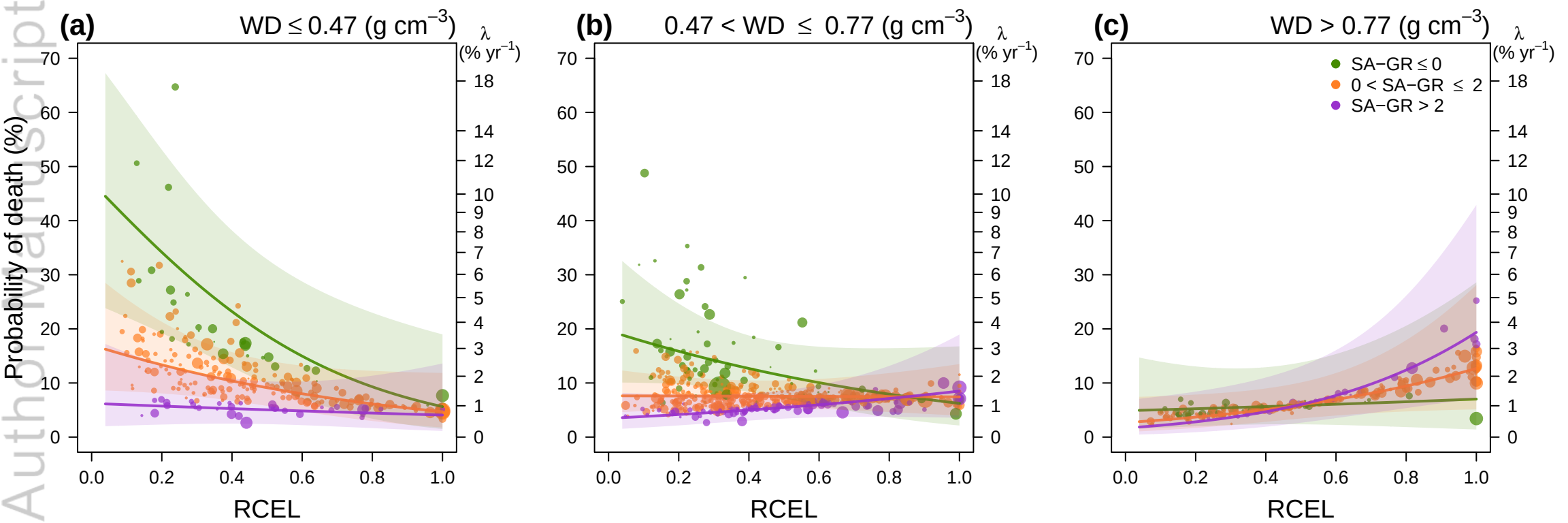

Author Manuscript